

# Ethanol steam reforming over Ni/ZnAl<sub>2</sub>O<sub>4</sub>-CeO<sub>2</sub>. Influence of calcination atmosphere and nature of catalytic precursor

Agustín E. Galetti, Manuel F. Gomez, Luis A. Arrua, M. Cristina Abello\*

Instituto de Investigaciones en Tecnología Química – (UNSL-CONICET), Chacabuco y Pedernera, (5700) San Luis, Argentina

## ARTICLE INFO

### Article history:

Received 13 July 2011

Received in revised form 6 September 2011

Accepted 11 September 2011

Available online 16 September 2011

### Keywords:

Ethanol steam reforming

Hydrogen production

Ni/ZnAl<sub>2</sub>O<sub>4</sub>-CeO<sub>2</sub> catalysts

## ABSTRACT

The hydrogen production from ethanol steam reforming has been studied over Ni/ZnAl<sub>2</sub>O<sub>4</sub>-CeO<sub>2</sub> catalysts. The influence of calcination atmosphere and nature of catalytic precursor was analyzed. The impregnation of Ni was carried out from two different nickel salts: nitrate (Nt) and acetate (Ac). The catalysts were obtained from the precursor calcination under reductive and oxidative atmospheres. The catalysts obtained from nitrate salt impregnation were the most carbon resistance measured as mmolC/mol reacted C<sub>2</sub>H<sub>5</sub>OH, and those obtained under a reductive atmosphere were the most stable, as evidenced by smaller activity losses. The Ni(Nt)/ZnAl<sub>2</sub>O<sub>4</sub>-CeO<sub>2</sub> obtained under reductive atmosphere was the most active (steady state ethanol conversion = 88%) and stable (activity loss = 14%) under mild reforming conditions (7.8% C<sub>2</sub>H<sub>5</sub>OH inlet concentration, H<sub>2</sub>O:C<sub>2</sub>H<sub>5</sub>OH molar ratio = 4.9, reaction temperature = 650 °C and W/F = 49 g min mol<sup>-1</sup><sub>C<sub>2</sub>H<sub>5</sub>OH</sub>). The hydrogen selectivity was 49% and the main C-containing products were CO<sub>2</sub>, CO and C<sub>2</sub>H<sub>4</sub>O.

© 2011 Elsevier B.V. All rights reserved.

## 1. Introduction

Ni catalysts have shown to be active and selective in the ethanol steam reforming reaction (ESR) for producing hydrogen [1–5]. The high C–C bond breaking activity and the relatively low cost compared to noble metals makes Ni a suitable active phase for ESR. The main problem for most of these catalytic systems is the high deactivation rate related to the formation of carbonaceous deposits and the sintering of metallic particles. The deactivation can occur by covering the active phase due to encapsulating carbon and also by filamentous carbon formation. There are many studies about the carbon formation on Ni systems [6–9] and a lot of effort has been focused on developing new Ni stable catalysts with improved resistance to coke formation. The morphology and chemical properties of carbon deposits depend on catalysts, operating conditions and the carbon source employed [10]. Thus, the carbon amounts are not only a function of time on stream but they also depend on the deposition and removing rates and reforming conditions.

The dopant addition and the modification of supports have been strategies used to increase the deactivation resistance since they could alter the carbon deposition rates and the catalyst properties. For instance, the addition of Ce and Pr to spinel type supports such as ZnAl<sub>2</sub>O<sub>4</sub> [11] and MgAl<sub>2</sub>O<sub>4</sub> [12] have shown an

improvement in the catalyst stability for decreasing the carbon amount and modifying its structure.

The Ni particle size and metallic dispersion are very important factors affecting the carbon deposition mechanism. It is well known that highly dispersed tiny particles avoid the carbon deposition, which could cause irreversible catalyst deactivation and/or the increase of catalytic bed pressure [13]. The metallic dispersion could be changed by using different precursors. Aupretre et al. [14] have prepared Rh/spinel catalysts supported on alumina by impregnation with rhodium nitrate, rhodium acetate or rhodium chloride. The metallic dispersion markedly increased by using nitrate and chloride. Besides, the authors claimed that the impregnation with acetate was very difficult and a significant part of the rhodium was not retained on the support. However, they reported that nitrate precursor should be avoided since less stable materials were produced due to their high acidity. Song et al. [15] have studied the effect of cobalt precursor on the performance of Co/CeO<sub>2</sub> catalysts. The best results were obtained by using organometallic Co precursors (especially cobalt acetyl acetonate) due to they increased the Co dispersion and the stability with a high H<sub>2</sub> yield. Llorca et al. [16] have also found differences in the performance of Co/ZnO catalysts for ESR depending on the cobalt-precursor. The catalyst prepared from Co<sub>2</sub>(CO)<sub>8</sub> showed the best performance due to a high degree of cobalt reduction with prevalence of small particles and the presence of a CoO phase.

In most of the works published, Ni catalysts were calcined in air and then reduced [1,17,18] at different temperatures and times before ESR reaction. These pretreatments could also lead to

\* Corresponding author.

E-mail address: [cabello@unsl.edu.ar](mailto:cabello@unsl.edu.ar) (M.C. Abello).

changes in particle sizes. Recently, Romero et al. [19] have reported the effect of activation treatments on Ni catalysts obtained from Ni(II)–Mg(II)–Al(III) layered double hydroxides. They have studied the effect of activation conditions over the surface and bulk properties and the catalytic performance in ethanol steam reforming. The catalysts obtained by calcination in air at 600 °C followed by reduction at 720 °C and those directly obtained from a precursor reduction at 720 °C showed the best performance under soft operating conditions (inlet ethanol molar fraction 2%, inert flow: 350 mL min<sup>-1</sup>, molar ratio H<sub>2</sub>O:C<sub>2</sub>H<sub>5</sub>OH = 5.5:1, diluted catalyst with an inert solid 1:10, no carbon formation). Lucreido et al. [20] have observed that the calcined Co/SiO<sub>2</sub> catalysts subjected to reduction displayed the smallest Co particle sizes. These authors have reported that the calcination stabilized the cobalt atoms in the SiO<sub>2</sub> structure preventing the Co<sup>0</sup> sintering. But the highest H<sub>2</sub> yield was obtained over the reduced catalyst prepared without calcination.

In a previous work, Ni catalysts supported over ZnAl<sub>2</sub>O<sub>4</sub> modified with Ce or Zr were examined [11] under mild operating conditions (high ethanol concentration into the feed, long time on stream, catalyst without dilution, low  $W/F_{C_2H_5OH}$ , and a H<sub>2</sub>O:C<sub>2</sub>H<sub>5</sub>OH molar ratio = 4.9). They were calcined in air a 700 °C and used in ESR without a previous reduction. The catalysts were stable at 650 °C during 35 h in time on stream. The main reaction products were H<sub>2</sub>, CO<sub>2</sub>, CO, C<sub>2</sub>H<sub>4</sub>O and small amounts of CH<sub>4</sub> and C<sub>2</sub>H<sub>4</sub>. The catalysts with Ce showed the best performance in reaction. The highest Ni<sup>2+</sup> dispersion and the high oxygen mobility from ceria or from Ni–Ce boundary allowed a higher residual activity and an improved coking resistance.

In this work, the effect of calcination atmosphere of catalytic precursor was studied over a Ni catalyst supported over ZnAl<sub>2</sub>O<sub>4</sub> modified by Ce addition. Furthermore, the influence of nickel source on the catalytic properties is also discussed. The catalyst submitted to different treatments was tested in ethanol steam reforming and it was characterized by N<sub>2</sub> physisorption, X-ray diffraction, temperature programmed reduction, thermogravimetry in oxidative atmosphere, scanning electron microscopy, Raman spectroscopy and H<sub>2</sub> chemisorption.

## 2. Experimental

### 2.1. Catalyst preparation

The support ZnAl<sub>2</sub>O<sub>4</sub>–CeO<sub>2</sub> with 10 wt.% of CeO<sub>2</sub> was prepared by sol–gel method reported elsewhere [11,21]. Briefly, it was synthesized by the hydrolysis of aluminium isopropoxide (AIP) and a molar ratio of 200 mol H<sub>2</sub>O/mol AIP at 95 °C. Then the solution of Zn(NO<sub>3</sub>)<sub>2</sub>·6H<sub>2</sub>O in isopropyl alcohol was added dropwise and finally, the Ce(NO<sub>3</sub>)<sub>3</sub>·6H<sub>2</sub>O aqueous solution, in the necessary amount to obtain a loading of 10 wt.% in Ce. After the addition of 0.7 mol H<sup>+</sup>/mol AIP, a transparent gel with low viscosity was obtained. The aging was carried out in a thermostatic bath at 65 °C overnight. The solid was dried at 110 °C for 10 h and decomposed in N<sub>2</sub> flow (100 mL min<sup>-1</sup>) under the following temperature program: from room temperature to 150 °C; at 150 °C for 2 h to eliminate the remained water; from 150 to 350 °C at a heating rate,  $\beta$ , of 5 °C min<sup>-1</sup>; at 350 °C for 2 h; from 350 to 500 °C at the same  $\beta$ ; at 500 °C for 5 h and then cooling to room temperature. Then, the solid was calcined at 700 °C under static air for 2 h to eliminate any carbonaceous residues and stabilize the support structure. The support was denoted as ZAC.

Four supported catalysts with 7 wt.% Ni were prepared by the incipient wetness impregnation technique using an aqueous solution of Ni(NO<sub>3</sub>)<sub>2</sub>·6H<sub>2</sub>O, (Nt), or Ni(CH<sub>3</sub>COO)<sub>2</sub>·4H<sub>2</sub>O, (Ac). After impregnation, the samples were dried at 90 °C for 6 h under

vacuum. The calcination was carried out at 600 °C at 10 °C min<sup>-1</sup> for 2 h under two different atmospheres:

- (i) Oxidative atmosphere, (O), in static air in oven.
- (ii) Reductive atmosphere, (R), in a 5% H<sub>2</sub>/N<sub>2</sub> flow (200 mL min<sup>-1</sup>).

The catalysts were denoted as ZAC–Y/X being Y:Ac or Nt indicative of Ni precursor and X:O or R indicative of calcination atmosphere. Thus, ZAC–Nt/R indicates a catalyst with 7 wt.% of Ni prepared from nitrate and calcined under a reductive atmosphere.

### 2.2. Catalyst characterization

All samples were characterized using different physical–chemical methods.

#### 2.2.1. Chemical composition

The chemical composition was performed by inductively coupled plasma-atomic emission spectroscopy (ICP) by using a sequential ICP spectrometer Baird ICP 2070 (BEDFORD, USA) with a Czerny Turner monochromator (1 m optical path). Alkali fusion with KHSO<sub>4</sub> and a subsequent dissolution with HCl solution brought the samples into solution

#### 2.2.2. BET surface area

BET surface areas were measured by using a Micromeritics Gemini V analyzer by adsorption of nitrogen at –196 °C on 200 mg of sample previously degassed at 240 °C for 16 h under flowing N<sub>2</sub>

#### 2.2.3. X-ray diffraction (XRD)

XR diffraction patterns were obtained with a RIGAKU diffractometer operated at 30 kV and 20 mA by using Ni-filtered Cu K $\alpha$  radiation ( $\lambda = 0.15418$  nm) at a rate of 3° min<sup>-1</sup> from  $2\theta = 20$ –80°. The powdered samples were analyzed without a previous treatment after deposition on a quartz sample holder. The identification of crystalline phases was made by matching with the JCPDS files.

#### 2.2.4. Thermal gravimetry (TG)

The analyzes were recorded by using DTG-60 Shimadzu equipment. The samples, ca. 15 mg, were placed in a Pt cell and heated from room temperature to 1000 °C at a heating rate of 10 °C min<sup>-1</sup> with a gas feed (air) of 50 mL min<sup>-1</sup>. Carbon deposited during reaction on used catalysts was evaluated as

$$\%C = \frac{w_{\text{coke}}}{w_{\text{final}}} \times 100$$

where  $w_{\text{coke}}$  is the coke mass deposited on the catalyst, calculated from the weight loss measured by TGA and  $w_{\text{final}}$  is the catalyst weight free of carbon remaining after the TG analysis.

#### 2.2.5. Differential thermal analysis (DTA)

These measurements were carried out at 10 °C min<sup>-1</sup> from room temperature to 1000 °C using a DTA-DTG-60 Shimadzu equipment.

#### 2.2.6. Temperature programmed reduction (TPR)

Studies were performed in a conventional TPR equipment. This apparatus consists of a gas handling system with mass flow controllers (Matheson), a tubular reactor, a linear temperature programmer (Omega, model CN 2010), a PC for data retrieval, a furnace and various cold traps. In most of the cases, the samples were oxidized in a 30 mL min<sup>-1</sup> flow of 20 vol.% O<sub>2</sub> in He at 300 °C for 30 min before each reduction run. After that, helium was admitted to remove oxygen and finally, the system was cooled to 25 °C. Some samples were only pre-treated in He at 300 °C for 30 min. The samples were subsequently contacted with a 30 mL min<sup>-1</sup> flow of 5 vol.% H<sub>2</sub> in N<sub>2</sub>, heated at a rate of 10 °C min<sup>-1</sup>, from 25 °C to a

final temperature of 700 °C and held at 700 °C for 1 h. Hydrogen consumption was monitored by a thermal conductivity detector after removing the formed water. The peak areas were calibrated with H<sub>2</sub> (5 vol%)/N<sub>2</sub> mixture injections

### 2.2.7. SEM-EDX

Scanning electron micrographs were obtained in a LEO 1450 VP. This instrument is equipped with an energy dispersive X-ray micro-analyzer, EDAX Genesis 2000 with Si(Li) detector which permitted analytical electron microscopy measurements. The samples were sputter coated with gold

### 2.2.8. Raman spectroscopy

The Raman spectra were recorded using a Lab Ram spectrometer (Jobin-Yvon) coupled to an Olympus confocal microscope (100× objective lens were used for simultaneous illumination and collection), equipped with a CCD with the detector cooled to about –70 °C using the Peltier effect. The excitation wavelength was in all the cases 532 nm (Spectra Physics argon-ion laser). The laser power was set at 30 mW. Integration times ranged from a few seconds to a few minutes depending on the sample. A scanning range between 100 and 2000 cm<sup>-1</sup> was applied

### 2.2.9. Hydrogen chemisorption

Nickel metal dispersion (*D%*) was determined by dual isotherm method. The samples were in situ reduced in pure H<sub>2</sub> at 600 °C for 60 min and the uptakes of strongly chemisorbed H<sub>2</sub> at 25 °C were measured between 5 and 100 Torr. A back-sorption isotherm was measured by repeating this procedure after evacuation at 500 °C for 30 min. The difference between chemisorption and back-sorption isotherms was used to estimate strongly chemisorbed hydrogen uptakes. A H/Ni titration stoichiometry equal to 1 was considered [22]. The reduced nickel surface area was estimated assuming a cross-sectional area of 0.065 nm<sup>2</sup> for a Ni atom and the average crystallite diameter was calculated for spherical particles [23].

### 2.3. Catalytic test

The ethanol steam reforming reaction was carried out in a stainless steel tube with an internal diameter of 4 mm operated at atmospheric pressure. The reactor was placed in a vertical furnace, which was controlled by a programmable temperature controller. The reaction temperature was measured with a coaxial K thermocouple. The feed to the reactor was a gas mixture of ethanol, water and helium (free of oxygen). Ethanol–water was fed to an evaporator (operated at 130 °C) through an isocratic pump operated at 0.15 mL min<sup>-1</sup>. The flow rates of gas stream were controlled by mass flowmeters. The experimental set-up was supplied with a low-pressure proportional relief valve for early detection of the plugged catalytic bed. The molar ratio in the feed was H<sub>2</sub>O: C<sub>2</sub>H<sub>5</sub>OH = 4.9 being the ethanol flow (*F*) 1.02 × 10<sup>-3</sup> mol min<sup>-1</sup> and 7.8% ethanol inlet concentration. The catalyst weight (*W*) was 50 mg (0.3–0.4 mm particle size range) without dilution. These experimental conditions were more severe than those usually found in literature. The catalyst was heated to reaction temperature under He flow, then the mixture with C<sub>2</sub>H<sub>5</sub>OH + H<sub>2</sub>O was allowed to enter into the reactor to carry out the catalytic test. In all the experiment runs, fresh samples were used. The reactants and reaction products were analyzed on-line by gas chromatography. H<sub>2</sub>, CH<sub>4</sub>, CO<sub>2</sub> and H<sub>2</sub>O were separated by a 1.8 m carbosphere (80–100 mesh) column and analyzed by TC detector. Nitrogen was used as an internal standard. Besides, CO was analyzed by a flame ionization detector after passing through a methanizer. Higher hydrocarbons and oxygenated products (C<sub>2</sub>H<sub>4</sub>O, C<sub>2</sub>H<sub>4</sub>, C<sub>2</sub>H<sub>6</sub>, C<sub>3</sub>H<sub>6</sub>O, C<sub>2</sub>H<sub>5</sub>OH, etc.) were separated in Rt-U PLOT capillary column and analyzed with FID using N<sub>2</sub> as carrier gas. The homogeneous contribution was tested

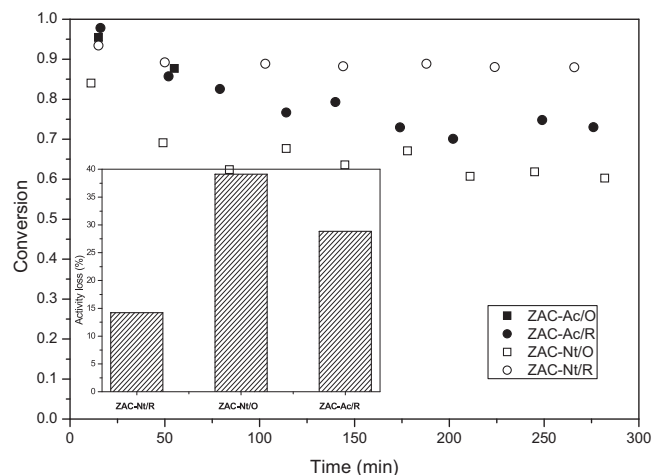


**Fig. 1.** Ethanol conversion as a function of time on stream over (●) ZAC-Ac/R; (■) ZAC-Ac/O; (○) ZAC-Nt/R; (□) ZAC-Nt/O. Reaction temperature = 650 °C; molar ratio = 4.9 mol<sub>H<sub>2</sub>O</sub>/mol<sub>C<sub>2</sub>H<sub>5</sub>OH</sub>; W/F = 49 g min mol<sub>C<sub>2</sub>H<sub>5</sub>OH</sub><sup>-1</sup>. Inset: activity loss for the same catalysts.

with the empty reactor. These runs showed an ethanol conversion lower than 1% at 650 °C.

Ethanol conversion (*X*<sub>EtOH</sub>), selectivity to carbon products (*S*<sub>i</sub>), hydrogen selectivity (*S*<sub>H<sub>2</sub></sub>) and activity loss (AL) were defined as follows

$$X_{\text{EtOH}} = \frac{F_{\text{EtOH}}^{\text{in}} - F_{\text{EtOH}}^{\text{out}}}{F_{\text{EtOH}}^{\text{in}}} \times 100$$

$$S_i = \frac{v_i F_i^{\text{out}}}{2(F_{\text{EtOH}}^{\text{in}} - F_{\text{EtOH}}^{\text{out}})} \times 100$$

$$S_{\text{H}_2} = \frac{F_{\text{H}_2}^{\text{out}}}{3(F_{\text{EtOH}}^{\text{in}} - F_{\text{EtOH}}^{\text{out}}) + (F_{\text{H}_2\text{O}}^{\text{in}} - F_{\text{H}_2\text{O}}^{\text{out}})} \times 100$$

$$\%AL = \frac{X_{\text{EtOH}}^0 - X_{\text{EtOH}}^{\text{SS}}}{X_{\text{EtOH}}^0} \times 100$$

*F*<sub>*i*</sub><sup>in</sup> and *F*<sub>*i*</sub><sup>out</sup> are the molar flow rates of product “*i*” at the inlet and outlet of the reactor, respectively, and *v*<sub>*i*</sub> is the number of carbon atoms in “*i*”. *X*<sub>EtOH</sub><sup>0</sup> and *X*<sub>EtOH</sub><sup>SS</sup> are the initial and steady state ethanol conversions.

## 3. Results and discussion

### 3.1. Catalytic activity under ethanol steam reforming

The performance of the four catalysts in ethanol steam reforming as a function of time is shown in Fig. 1. All the results are shown up to 300 min in time on stream except for ZAC-Ac/O. The experimental run over this last sample is interrupted after 140 min due to the increase of reactor pressure bed. All catalysts as prepared (without pre-treatment) are active with a complete initial ethanol conversion that decreases until almost 150 min. After this long induction period, a pseudo-steady state regimen is reached with the activity order ZAC-Nt/R (*X*<sub>EtOH</sub><sup>SS</sup> = 88%) > ZAC-Ac/R (*X*<sub>EtOH</sub><sup>SS</sup> = 74%) > ZAC-Nt/O (*X*<sub>EtOH</sub><sup>SS</sup> = 63%). The activity loss data are also presented in Fig. 1 and follows the order ZAC-Nt/R (%AL = 14.2%) > ZAC-Ac/R (%AL = 28.8%) > ZAC-Nt/O (%AL = 39.1). The ZAC-Nt/R is the most stable catalyst, as evidenced by a smaller activity loss. The main products are H<sub>2</sub>, CO<sub>2</sub>, CO and C<sub>2</sub>H<sub>4</sub>O, Fig. 2. For ZAC-Nt/R, ZAC-Ac/R and ZAC-Nt/O, CH<sub>4</sub> and C<sub>2</sub> (C<sub>2</sub>H<sub>4</sub> + C<sub>2</sub>H<sub>6</sub>) compounds are

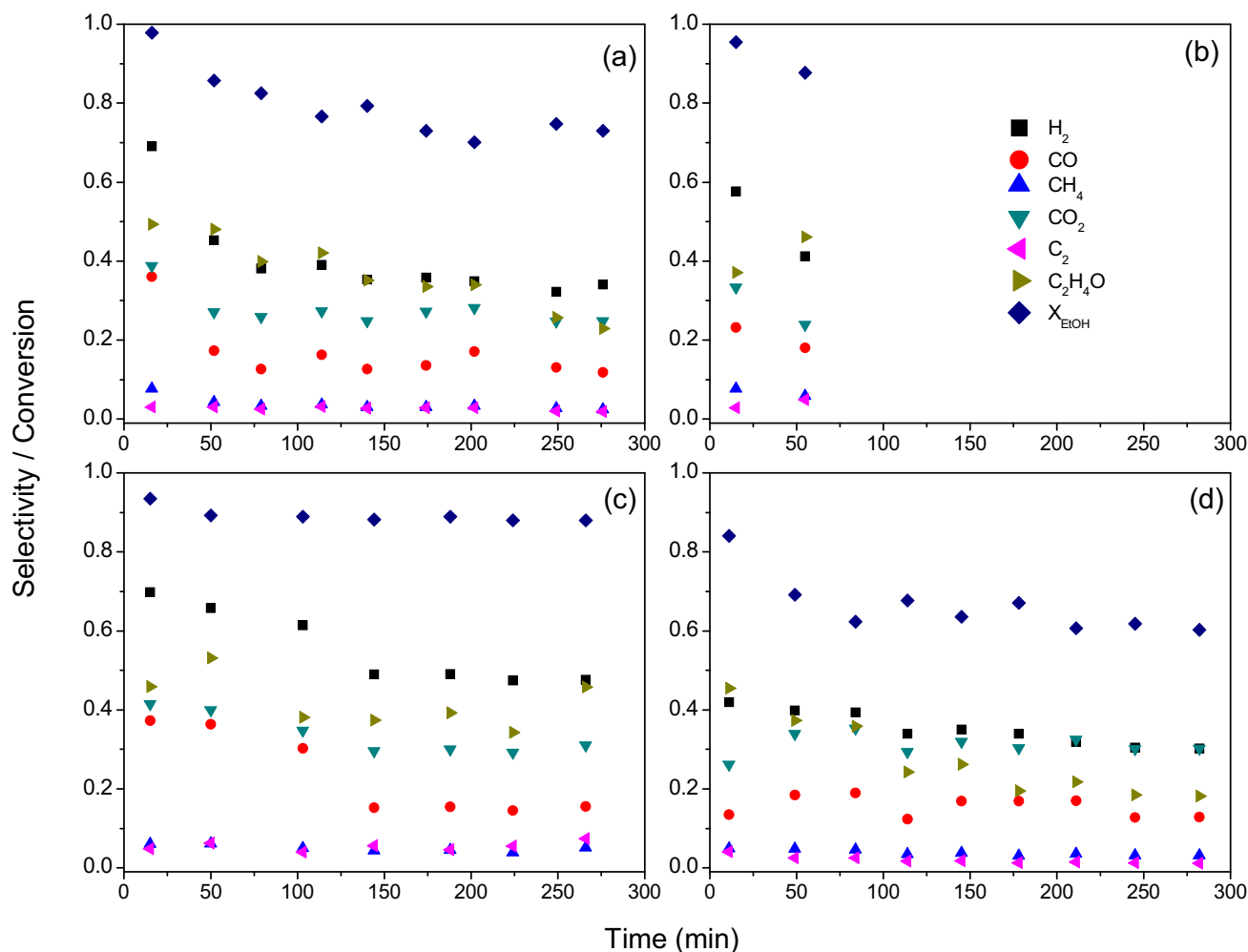


**Fig. 2.** Product distribution and activity in ethanol steam reforming over (a) ZAC-Ac/R; (b) ZAC-Ac/O; (c) ZAC-Nt/R; (d) ZAC-Nt/O. Treaction temperature = 650 °C; molar ratio = 4.9 mol<sub>H<sub>2</sub>O</sub>/mol<sub>C<sub>2</sub>H<sub>5</sub>OH</sub>; W/F = 49 g min mol<sub>C<sub>2</sub>H<sub>5</sub>OH</sub><sup>-1</sup>.

observed in minor amounts with selectivities below 5%. The hydrogen selectivity follows the same order as conversion: ZAC-Nt/R ( $S_{H_2} = 49\%$ ) > ZAC-Ac/R ( $S_{H_2} = 34\%$ ) > ZAC-Nt/O ( $S_{H_2} = 31\%$ ). After the transitory period, the CO/CO<sub>2</sub> molar ratios are similar and ranged between 0.48 and 0.53. In a previous work, a catalyst prepared as ZAC-Nt/O but calcined in air at 700 °C showed a slightly lower conversion but a similar hydrogen selectivity [11]. The results presented in this work correspond to a new catalyst batch, therefore it can be suggested that the preparation method is fairly reproducible. The ZAC-Ac/O sample shows the highest C–C breaking capacity as regarding the initial acetaldehyde formation, which is the lowest. In fact over this catalyst the reactor temperature decreases 30 °C when the ethanol–water feed enter into the reactor. The decrease in conversion is accompanied with the decrease in H<sub>2</sub>, CO<sub>2</sub>, CO and CH<sub>4</sub> selectivities whereas C<sub>2</sub>H<sub>4</sub>O and C<sub>2</sub> selectivities increase, suggesting that this catalyst rapidly loses its cracking activity with the time on stream. A high carbon deposition rate could be inferred on this sample leading to the reactor plugging.

### 3.2. Characterization of catalysts

Some characteristics of catalysts are shown in Table 1. The specific surface areas are between 35 and 41 m<sup>2</sup> g<sup>-1</sup>. The Ni impregnation slightly decreases the  $S_{BET}$  in comparison with the support ( $S_{BET} = 42$  m<sup>2</sup> g<sup>-1</sup>) and it can be suggested that the decrease is

slightly higher in the catalysts where the nitrate salt was used as Ni source.

In the diffraction patterns of fresh samples, Fig. 3, the reflection lines corresponding to ZnAl<sub>2</sub>O<sub>4</sub> ( $2\theta = 31.3^\circ, 36.8^\circ, 44.8^\circ, 55.6^\circ, 59.4^\circ$  and  $65.3^\circ$ , JCPDS-5-669) and CeO<sub>2</sub> ( $2\theta = 28.5^\circ, 33.3^\circ, 47.5^\circ, 56.3^\circ$ , JCPDS 30-0394) are observed. For the ZAC-Ac/R sample obtained under reductive atmosphere, broad peaks of Ni<sup>0</sup> ( $44.5^\circ, 51.8^\circ$ , JCPDS 4-0850) are detected. However, the reflection lines of Ni compounds or Ni<sup>0</sup> are almost undetectable for ZAC-Nt/R, suggesting a higher nickel dispersion and/or size particles lower than 4 nm. For the samples obtained in oxidative atmosphere the peaks assigned to NiO at  $2\theta = 43.3^\circ, 62.9^\circ$  (JCPDS 4-835) are clearly observed. The intensities of these peaks are markedly higher for ZAC-Ac/O. The particle size of NiO determined by Scherrer follows the order ZAC-Ac/O > ZAC-Nt/O. Since reflections of NiAl<sub>2</sub>O<sub>4</sub> are coincident to ZnAl<sub>2</sub>O<sub>4</sub>, its presence cannot be ruled out. The ZnAl<sub>2</sub>O<sub>4</sub> used as support is a highly stabilized spinel and the Ni impregnation was carried out in successive steps by dry impregnation method, consequently the stoichiometric NiAl<sub>2</sub>O<sub>4</sub> formation should be very low. However, nickel could be incorporated into the subsurface of the zinc spinel, and a surface Ni compound related to Ni strongly interacting with spinel matrix could be formed.

Fig. 4 exhibits XRD patterns for used samples. They show the diffraction lines corresponding to the modified support and Ni<sup>0</sup>. Besides, in all the samples the reflection line (002) corresponding to graphitic carbon is detected ( $2\theta = 26.4^\circ$ , JCPDS 41-1487).

**Table 1**  
Some characteristics of fresh catalysts.

Sample	Chemical composition <sup>a</sup> (wt%)				$S_{\text{BET}}$ ( $\text{m}^2 \text{g}^{-1}$ )	$D\%$	$d_{\text{Ni}}$ (nm)
	Ni	Ce	Zn	Al			
ZAC-Nt/R	5.47	10.52	16.2	13.0	37	1.95	52
ZAC-Ac/R	5.46	11.53	17.6	13.5	41	2.20	46
ZAC-Nt/O	5.47	10.52	16.2	13.0	35	1.67	60
ZAC-Ac/O	5.46	11.53	17.6	13.5	39	1.43	71

$S_{\text{BET}}$  for ZAC support:  $42 \text{ m}^2 \text{ g}^{-1}$ .

<sup>a</sup> Values determined by ICP.

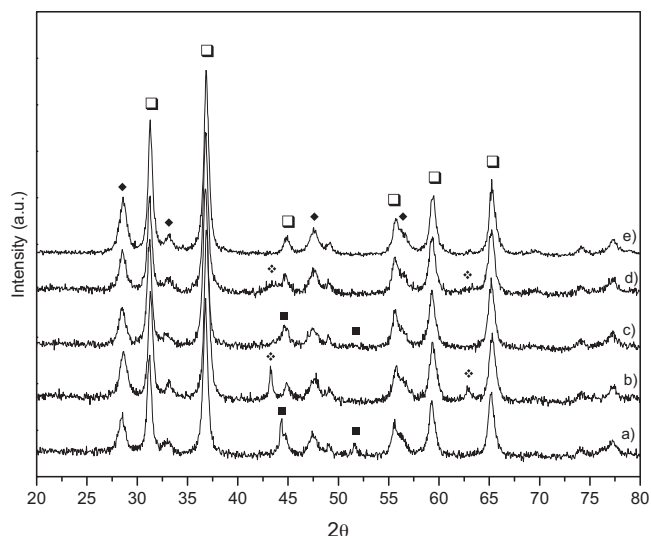


**Fig. 3.** X-ray diffraction patterns of fresh samples (a) ZAC-Ac/R; (b) ZAC-Ac/O; (c) ZAC-Nt/R; (d) ZAC-Nt/O; (e) ZAC. (□)  $\text{Zn Al}_2\text{O}_4$ , (◆)  $\text{CeO}_2$ , (■) Ni, (◆) NiO.

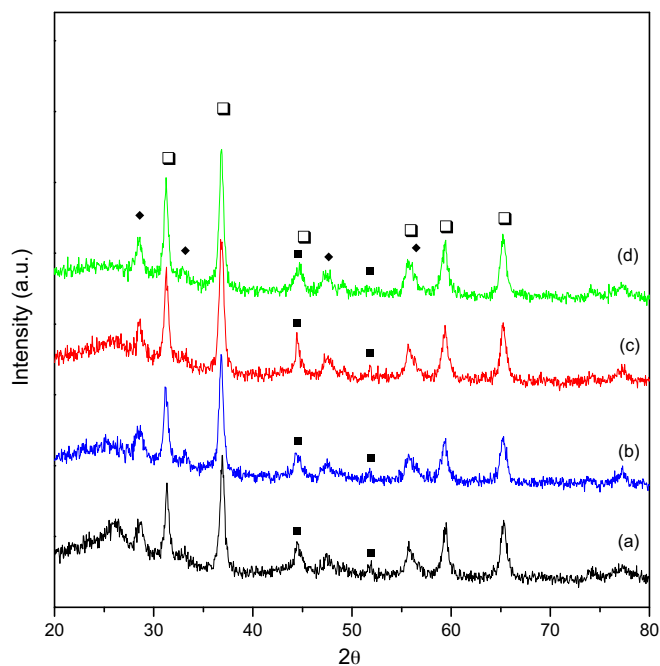


**Fig. 4.** X-ray diffraction patterns of used samples: (a) ZAC-Ac/O; (b) ZAC-Nt/O; (c) ZAC-Ac/R; (d) ZAC-Nt/R. (□)  $\text{Zn Al}_2\text{O}_4$ , (◆)  $\text{CeO}_2$ , (■) Ni, (□) graphite C.

The intensity of this peak follows the order of  $\text{ZAC-Ac/O} > \text{ZAC-Ac/R} > \text{ZAC-Nt/O} > \text{ZAC-Nt/R}$  in agreement with the carbon amount

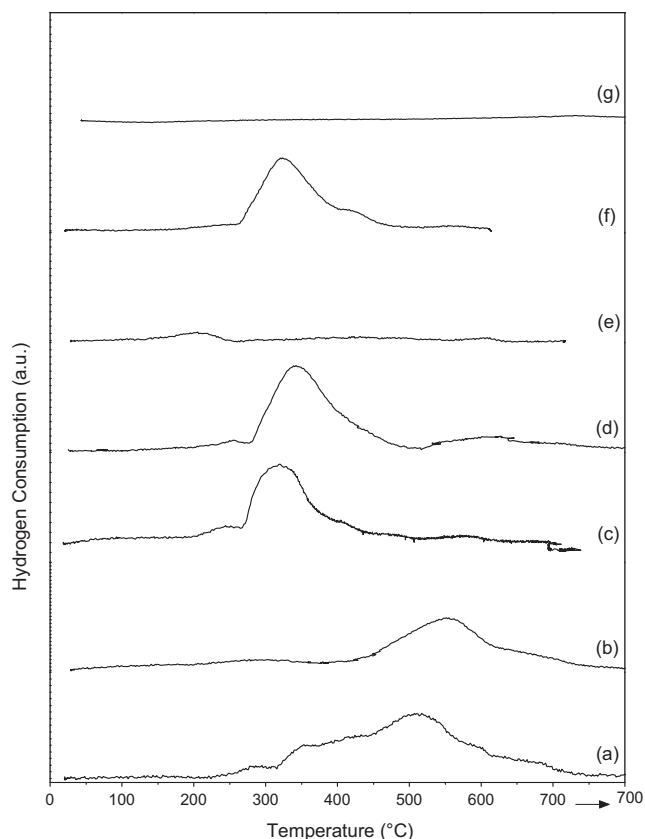


**Fig. 5.** Temperature programmed reduction of (a) ZAC-Ac/O; (b) ZAC-Nt/O; (c) ZAC-Ac/R (after  $\text{O}_2$  pretreatment); (d) ZAC-Nt/R (after  $\text{O}_2$  pretreatment); (e) ZAC-Ac/R (after He pretreatment); (f) ZAC-Nt/R (after He pretreatment); (g) ZAC-Nt/R (in situ precursor reduction).

determined by TG-TPO experiments and SEM observations (see further).

In Fig. 5, the temperature programmed reduction profiles are shown. In curves (a and b) the TPR profiles for catalysts obtained under an oxidative atmosphere are illustrated. In both cases a  $\text{H}_2$  uptake at low temperatures (around  $280^\circ\text{C}$ ) could be assigned to a partial reduction of  $\text{CeO}_2$  surface oxygen [11] and to the reduction of weakly interacted NiO with the spinel support. For ZAC-Ac/O, a  $\text{H}_2$  uptake peak is observed up to  $320^\circ\text{C}$ . The shoulder at  $384^\circ\text{C}$  is attributed to NiO reduction whereas the peak at  $515^\circ\text{C}$  could be assigned to  $\text{Ni}^{2+}$  reduction with a high degree of interaction with the modified support. For ZAC-Nt/O, the high temperature  $\text{H}_2$  uptake peak is centered at  $565^\circ\text{C}$  and again it is assigned to the  $\text{Ni}^{2+}$  reduction with a high degree of interaction with the modified support. This last profile is very similar to that reported in Ref. [11]. The difference in the maximum temperature is due to differences in TPR conditions. The TPR profiles for samples obtained under reductive atmosphere are shown in Fig. 5, curves c–f. When the samples are pre-treated in oxygen at  $300^\circ\text{C}$  before TPR experiment, curves c

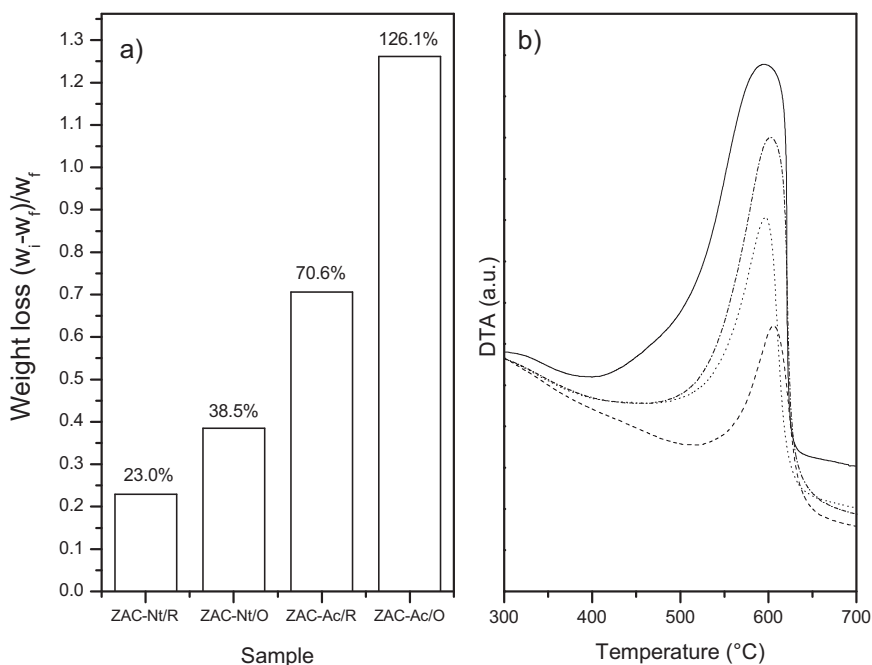


Fig. 6. TG–DTA analysis of used catalysts under reforming. (a) Weight loss and (b) DTA. — ZAC-Ac/O; - - - - ZAC-Ac/R; - - - ZAC-Nt/R; ···· ZAC-Nt/O.

and d, similar profiles are obtained for both samples, ZAC-Nt/R and ZAC-Ac/R, with maximum temperature peaks at 340 and 330 °C, respectively. These peaks correspond to NiO reduction (pure NiO reduces around 360 °C under the same reduction conditions [7,24]). The small peaks at 240 °C could be again attributed to reduction of surface CeO<sub>2</sub>. When the samples are pre-treated in He at 300 °C, the ZAC-Ac/R sample only shows the peak corresponding to reduction of ceria, suggesting that the Ni<sup>0</sup> species are very stable which is in agreement with XRD, Fig. 3. However, a H<sub>2</sub> consumption peak at 321 °C is clearly observed in the TPR profile for ZAC-Nt/R. This unexpected result could indicate that very tiny Ni<sup>0</sup> particles generated during precursor calcination are very reactive. They become oxidized by contact with atmosphere during the air exposure or with oxygen from CeO<sub>2</sub> during pre-treatment (but they are not detected by XRD, Fig. 3). This could have consequences under reforming conditions. When the TPR experiment is carried out over in situ pre-treated precursor sample under reductive atmosphere, an almost flat profile is obtained, curve g. From this result, it could be inferred that the precursor calcination under reductive atmosphere leads to a complete reduction of nickel species and they could be oxidized by the air exposure or by oxygen from ceria. TPR results reveal that the calcination atmosphere affects the metal-support interactions. These interactions are stronger on catalysts prepared under oxidative atmosphere causing the peaks to shift to higher temperature.

The Ni dispersion on reduced samples determined by H<sub>2</sub> chemisorption is shown in Table 1. The catalysts are poorly dispersed. The dispersion follows the order: ZAC-Ac/R > ZAC-Nt/R > ZAC-Nt/O > ZAC-Ac/O. Nickel particle sizes of ZAC-Ac/R and

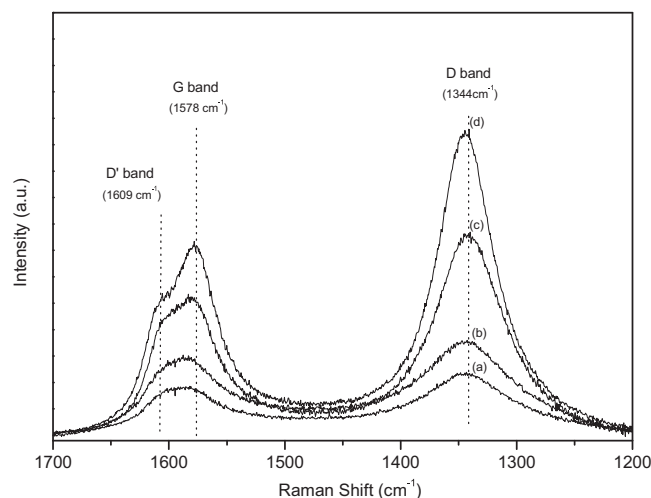


Fig. 7. Raman spectra of catalysts after being used in ethanol steam reforming reaction (a) ZAC-Ac/O; (b) ZAC-Ac/R; (c) ZAC-Nt/R; (d) ZAC-Nt/O.

ZAC-Nt/R catalysts are very close and lower than those of ZAC-Ac/O and ZAC-Nt/O. The slightly smaller value for ZAC-Ac/R could be related to the higher stability of Ni particles as it was observed by XRD. As mentioned above, the Ni<sup>0</sup> particles formed over ZAC-Nt/R can be oxidized during air exposure or by oxygen from CeO<sub>2</sub> and then they could be sintered by the reduction at 600 °C for 60 min in the H<sub>2</sub> chemisorption experiment. If the same

**Table 2**  
Characteristics of carbon deposits after ethanol steam reforming.

Sample	$T_{\max}$ TG–DTA (°C)	%C TPO	$X_{\text{av}}$	mmolC/mol reformed C <sub>2</sub> O <sub>5</sub> OH	Raman $I_D/I_G$
ZAC-Nt/R	605.7	23	0.89	3.5	1.34
ZAC-Ac/R	602.2	70.6	0.66	14.6	1.20
ZAC-Nt/O	596.8	38.5	0.79	6.6	1.54
ZAC-Ac/O	596.2	128	0.93 <sup>a</sup>	–	1.15

$X_{\text{av}}$  average ethanol conversion.

<sup>a</sup> Value at 55 min.

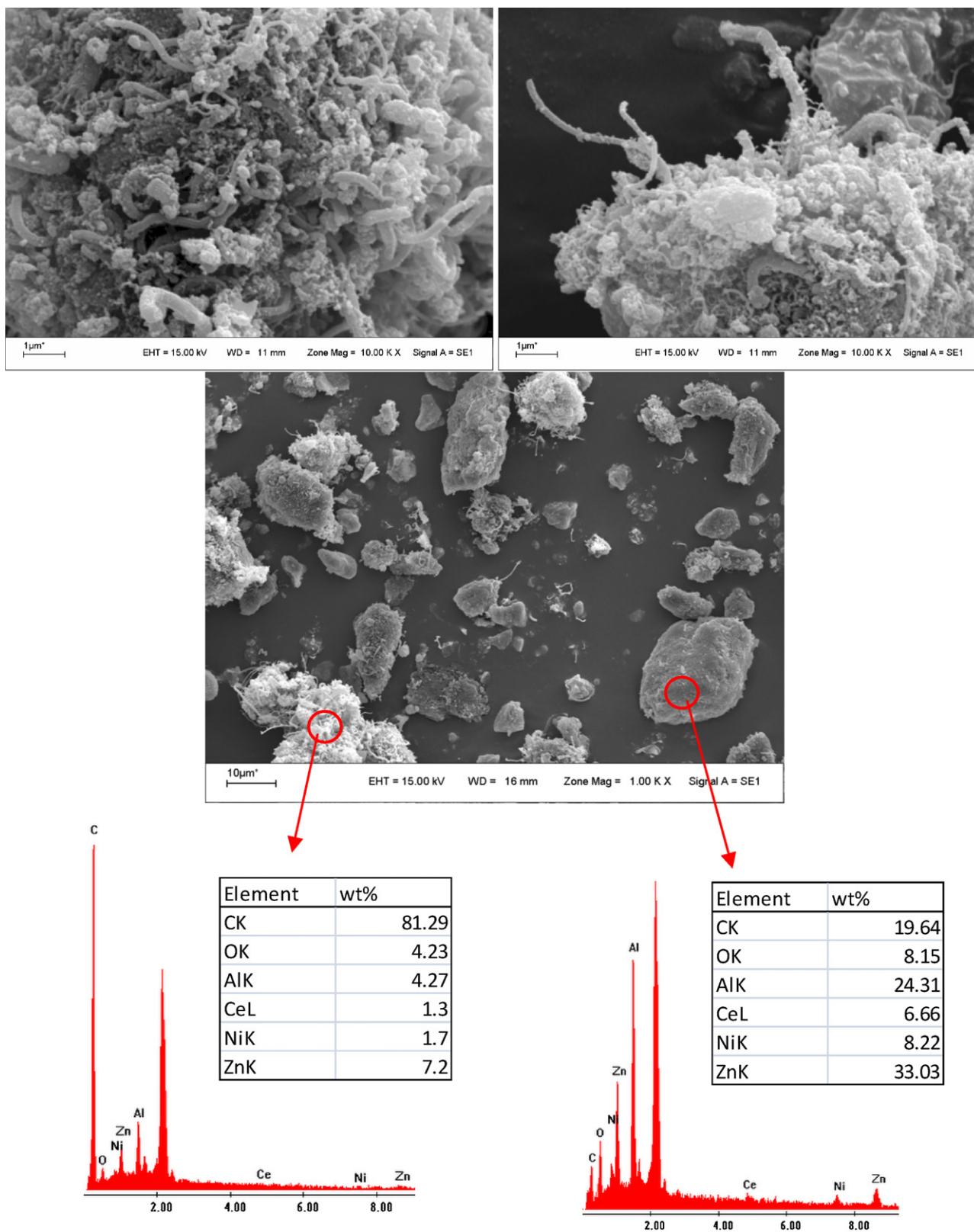


Fig. 8. SEM micrographs and EDX spectra of ZAC-Ac/R after being used in ethanol steam reforming reaction.

precursor is compared under different atmosphere treatments, in both cases the dispersion increases under reductive atmosphere (in 17% on ZAC-Nt/R and in 54% on ZAC-Ac/R). For ZAC-Ac/R the value obtained by Scherrer equation is 25 nm which is markedly lower

than that estimated by  $H_2$  chemisorption (46 nm). Although there is an uncertainty in the particle size determined by XRD, it could be inferred that the reduction treatment before  $H_2$  chemisorption should favor the particle sintering. Concerning the ESR reaction, the

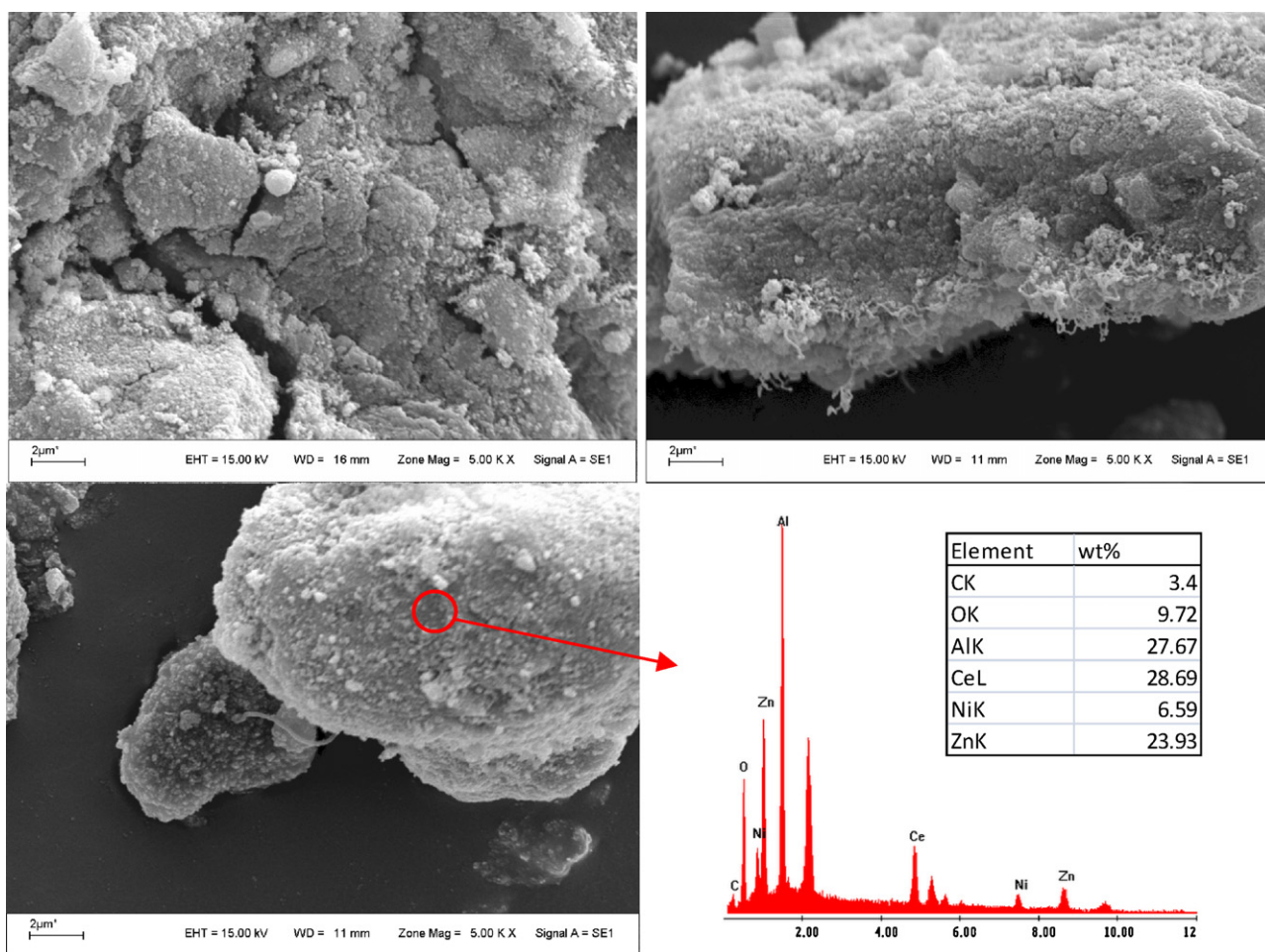


Fig. 9. SEM micrographs and EDX spectra of ZAC-Nt/R after being used in ethanol steam reforming reaction.

H<sub>2</sub> selectivity is the greatest for samples, which were subjected to the reductive calcination. Additionally, these samples exhibit the highest stability.

The DTA analyzes for the used samples for 300 min in ethanol steam reforming (except for ZCA-Ac/O used for 140 min) are presented in Fig. 6. In all samples an intense and broad exothermic peak at 400–650 °C is observed, Table 2. In the catalysts obtained in a reductive atmosphere, the exothermic peak slightly shifted to high temperature. A slight increase in the maximum oxidation temperature is observed on ZAC-Nt/R sample, indicating that the carbon deposits, even though significantly less in absolute amount, are slightly less reactive. It is well known that the usual graphitic or filamentous coke is oxidized at temperatures higher than 500 °C [2]. In Fig. 6(a) and Table 2, the carbon amounts determined by TG-TPO are shown. The values follow the order ZAC-Nt/R (%C = 23) < ZAC-Nt/O (%C = 38.5) < ZAC-Ac/R (%C = 70.6%) < ZAC-Ac/O (%C = 128.1) which is not the same as the steady state conversion value (ZAC-Nt/R ( $X_{\text{EtOH}}^{\text{SS}} = 88\%$ ) > ZAC-Ac/R ( $X_{\text{EtOH}}^{\text{SS}} = 74\%$ ) > ZAC-Nt/O ( $X_{\text{EtOH}}^{\text{SS}} = 63\%$ )) neither the activity loss order (ZAC-Nt/R (%AL = 14.2) > ZAC-Ac/R (%AL = 28.8) > ZAC-Nt/O (%AL = 39.1)).

The nature and characteristics of carbon deposits are also studied by Raman spectroscopy. In Fig. 7, the Raman spectra of used samples are shown in the range of 1200–1700 cm<sup>-1</sup>. In all the cases, two broad bands centered at ~1578 cm<sup>-1</sup> (G band) and 1344 cm<sup>-1</sup> (D band) are observed. They are attributed to the stretching mode of carbon sp<sup>2</sup> bonds of the typical graphite and to the vibrations of carbon atoms in disordered graphite planes, respectively. In all

the cases, the D band intensity is higher than that of G band. The  $I_{\text{D}}/I_{\text{G}}$  intensity ratio shown in Table 2 follows the order of ZAC-Nt/O > ZAC-Nt/R > ZAC-Ac/R > ZAC-Ac/O. Then, it could be inferred that over the samples obtained from nitrate salt there is a higher amount of disordered structures [25]. Besides, on samples obtained from nitrate salt a defect-related Raman band is clearly observed at 1609 cm<sup>-1</sup> known as D' band [26,27]. This band is usually associated with “in plane” defects which break the translational symmetry of the graphene sheet [28]. The Nj particle properties such as size, shape or interaction degree with the catalytic support can modify the stacking pattern of graphene planes during the carbonaceous deposit formation.

The presence of carbon deposits over the catalysts prepared under reductive atmosphere is also examined by SEM. Fig. 8 shows the SEM micrographs for ZAC-Ac/R catalyst after reaction. The formation of an abundant amount of filaments with a great heterogeneity in diameter and length is observed. It is likely that the metal sites remain uncovered on the filament tips despite the large amount of carbon (70.6%) without presenting an immediate deactivation. The EDX analysis on different particles reveals a no homogeneous distribution of carbon deposits. For ZAC-Nt/R catalyst, Fig. 9, after an exhaustive examination of several particles, the filament formation is much lower and the filament diameters are markedly smaller.

As it was mentioned all catalysts are initially very active (ethanol conversion 100%) but the highest deactivation is for ZAC-Ac/O catalyst. For this sample the formation of large diameter filaments

(the Ni particle diameter is the highest) and encapsulating carbon could be inferred. The Raman intensity ratio ( $I_D/I_G = 1.15$ , Table 2) is also indicating the presence of an important graphitic carbon fraction. Besides, over this catalyst the reduction of Ni particles and the carbon deposition simultaneously occur and this simultaneity should modify the carbon nature.

Wang and Lu [29] have reported the activities of Ni/ $\gamma$ -Al<sub>2</sub>O<sub>3</sub> catalysts prepared from different nickel precursors in the dry methane reforming reaction. The nitrate-derived catalyst exhibited higher activity and stability than those prepared from nickel chloride and nickel acetylacetonate. The carbon deposition on catalysts derived from inorganic precursors (nitrate and chloride) was more severe than on the organic precursor-derived catalyst. The authors claimed that the active carbon species (–C–C–) from the resulting graphitic structures on the Ni nitrate-derived catalyst were responsible of the highest stability. In contrast, the carbon formed on Ni acetylacetonate-derived catalyst was dominated by inactive species –CO–C– species which leading to a more severe deactivation.

The carbon deposition rate on ZAC-Y/X catalysts could be the same at the beginning of the reaction (ethanol conversions are the same for the four samples) but the carbon growing steps (carbon diffusion through the particle, surface diffusion, the nucleation rate and formation of graphitic layers) should be different as it is evidenced by Raman, TG-TPO and SEM. Comparing nitrate and acetate Ni source, it is revealed that the use of acetate does not provide advantages. As it was mentioned, Ni<sup>0</sup> particles formed on ZAC-Nt/R suffer a re-oxidation by air or from CeO<sub>2</sub> during the previous He heating in the ESR. They could have a surface structure different to those generated on ZAC-Ac/R, which could explain the differences in catalytic behavior. It is well known that the dissociation rate of a carbon-containing gas and the carbon growth process depend on the detailed surface structure of metal among other factors [30]. However, this hypothesis cannot be conclusively confirmed based on the available experimental data.

In summary, the samples prepared from a nitrate solution produce lower amounts of carbon than those obtained from an acetate solution. Besides, the calcination under reductive atmosphere leads to a better dispersion and smaller metallic particle sizes. The samples prepared under an oxidative atmosphere are less stable (higher activity loss) than those under a reductive due likely to the simultaneity of nickel reduction and carbon deposition processes.

#### 4. Conclusions

The influence of calcination atmosphere and nature of catalytic precursor over Ni/ZnAl<sub>2</sub>O<sub>4</sub>-CeO<sub>2</sub> catalysts in the ethanol steam reforming reaction was studied. The catalysts obtained from nitrate salt impregnation were the most carbon resistance, and those obtained under reductive atmosphere were the most stable, as evidenced by smaller activity losses. The use of acetate solution as Ni source does not provide advantages due to the graphitic carbon fractions formed by reaction were more resistance to be

removed under reforming conditions. The Ni(Nt)/ZnAl<sub>2</sub>O<sub>4</sub>-CeO<sub>2</sub> obtained under reductive atmosphere was the most active (steady state ethanol conversion = 88%) and stable (activity loss = 14%) under mild reforming conditions (7.8% ethanol inlet concentration, H<sub>2</sub>O:C<sub>2</sub>H<sub>5</sub>OH molar ratio = 4.9, reaction temperature = 650 °C and W/F = 49 g min mol<sup>-1</sup>C<sub>2</sub>H<sub>5</sub>OH<sup>-1</sup>). The hydrogen selectivity was 49% and the main C-containing products were CO<sub>2</sub>, CO and C<sub>2</sub>H<sub>4</sub>O.

#### Acknowledgments

Financial supports are acknowledged to CONICET, ANPCyT and Universidad Nacional de San Luis. The authors wish to thank Dr. John Múnera for Raman assistance. The funds from the ANPCyT to buy the Raman instrument are also grateful (PME 87-PAE 36985).

#### References

- [1] Prakash Biswas, Deepak Kunzru, Int. J. Hydrogen Energy 32 (2007) 969–980.
- [2] M.C. Sánchez-Sánchez, R.M. Navarro, J.L.G. Fierro, Int. J. Hydrogen Energy 32 (2007) 1462–1471.
- [3] F. Frusteri, S. Freni, V. Chiodo, L. Spadaro, O. Di Blasi, G. Bonura, S. Cavallaro, Appl. Catal. A 270 (2004) 1–7.
- [4] J.W.C. Liberatori, R.U. Ribeiro, D. Zanchet, F.B. Noronha, J.M.C. Bueno, Appl. Catal. A 327 (2007) 197–204.
- [5] J. Comas, F. Mariño, M. Laborde, N. Amadeo, Chem. Eng. J 98 (2004) 61–68.
- [6] A. Galetti, M. Gomez, L. Arrua, A. Marchi, M.C. Abello, Catal. Commun. 9 (2008) 1201–1208.
- [7] A. Galetti, M. Gomez, L. Arrua, M.C. Abello, Appl. Catal. A 348 (2008) 94–102.
- [8] A. Vizcaíno, P. Arena, G. Baronetti, A. Carrero, J. Calles, M. Laborde, N. Amadeo, Int. J. Hydrogen Energy 33 (2008) 3489–3492.
- [9] A.L. Alberton, M.M. Souza, M. Schmal, Catal. Today 123 (2007) 257–264.
- [10] X. Chen, A.R. Tadd, J.W. Schwank, J. Catal. 251 (2007) 374–387.
- [11] A. Galetti, M. Gomez, L. Arrua, M.C. Abello, Appl. Catal. A 380 (2010) 40–47.
- [12] M.N. Barroso, A.E. Galetti, M.C. Abello, Appl. Catal. A 394 (2011) 124–131.
- [13] A. Effendi, Z.G. Zhang, K. Hellgardt, K. Honda, T. Yoshida, Catal. Today 77 (2002) 181–189.
- [14] F. Aupretre, C. Descorme, D. Duprez, D. Casanave, D. Uzio, J. Catal. 233 (2005) 464–477.
- [15] H. Song, B. Mirkelamoglu, U. Oskan, Appl. Catal. A 382 (2010) 58–64.
- [16] J. Llorca, P. Ramírez de la Piscina, J.A. Dalmon, J. Sales, N. Homs, Appl. Catal. A 43 (2003) 355–369.
- [17] A.J. Vizcaíno, A. Carrero, J.A. Calles, Int. J. Hydrogen Energy 32 (2007) 1450–1461.
- [18] F. Wang, Y. Li, W. Cai, E. Zhan, X. Mu, W. Shen, Catal. Today 146 (2009) 31–36.
- [19] A. Romero, M. Jobbagy, M. Laborde, G. Baronetti, N. Amadeo, Catal. Today 149 (2010) 407–412.
- [20] A.F. Lucreido, J.D.A. Bellido, A. Zawadzki, E.M. Assaf, Fuel 90 (2011) 1424–1430.
- [21] B. Yoldas, Ceram. Bull. 54 (3) (1975) 289–290.
- [22] M.C.J. Bradford, M.A. Vannice, Appl. Catal. A 142 (1996) 97–122.
- [23] J.S. Smith, P.A. Thrower, M.A. Vannice, J. Catal. 68 (1981) 270–285.
- [24] M.N. Barroso, M. Gomez, L. Arrua, M.C. Abello, Appl. Catal. A 304 (2006) 116–123.
- [25] F. Pompeo, N. Nichio, O. Ferretti, D. Resasco, Int. J. Hydrogen Energy 30 (2005) 1399–1405.
- [26] S. Maldonado, S. Morin, K.J. Stevenson, Carbon 44 (2006) 1429–1437.
- [27] L.M. Cornaglia, J. Múnera, S. Irusta, E.A. Lombardo, Appl. Catal. A 263 (2004) 91–101.
- [28] E.B. Barros, A.G. Souza Filho, H. Son, M.S. Dresselhaus, Vib. Spectrosc. 45 (2007) 122–127.
- [29] S. Wang, G.Q. Lu, Appl. Catal. A 169 (1998) 271–280.
- [30] M.L. Toebes, J.H. Bitter, A. Jos van Dillen, K.P. de Jong, Catal. Today 76 (2001) 33–42.